Synthesis and photophysical properties of "center-to-edge" type phosphorus(v) porphyrin arrays

Kimihiro Susumu,[a] Kazuyoshi Tanaka,*[a] Takeo Shimidzu,[a] Yasuko Takeuchi[b] and Hiroshi Segawa *[bc]

[a] *Department of Molecular Engineering, Graduate School of Engineering, Kyoto University, Sakyo-ku, Kyoto 606-8501, Japan*
[b] *Department of Chemistry, Graduate School of Arts and Sciences, The University of Tokyo, 3-8-1 Komaba, Meguro-ku, Tokyo 153-8902, Japan*
[c] *"Field and Reaction", PRESTO, Japan Science and Technology Corporation (JST), Japan*

Received (in Cambridge) 17th December 1998, Revised 21st April 1999, Accepted 27th April 1999

The synthesis, characterization and photophysical properties of a series of "center-to-edge" type phosphorus(v) porphyrin arrays in which the *central* phosphorus atom of one phosphorus(v) porphyrin is connected to the *meso*-phenoxy *edge* of the other phosphorus(v) porphyrin(s) are described. The conformation of the porphyrin arrays is estimated from the NMR data on the basis of the porphyrin ring current model. From the structural assignments and absorption properties of the arrays it is suggested that the electronic coupling between the porphyrin rings in the arrays is small. Nevertheless, solvent-polarity dependence of the excited-state properties indicates an enhancement of the nonradiative decay *via* the charge transfer state.

Introduction

Construction of artificial multi-porphyrin systems is an intriguing subject in relation to the natural photosynthetic systems such as the light-harvesting complexes and the photosynthetic reaction center. In order to mimic both the excitation energy transfer in the light-harvesting complexes and the photoinduced electron transfer in the reaction center, various types of multi-porphyrin systems have been synthesized and investigated.[1–14] Understanding the functions of ultrafast energy or electron transfer processes enable us to utilize them as molecular photonic devices in which a photon initiates the process.[15,16] The key elements of the natural photosynthetic systems include the efficient collection of solar energy by the light-harvesting antenna, the quantitative energy transfer to the special pair of the reaction center, and the rapid and unidirectional charge separation in the electron-transfer chain of the reaction center.[17–19] In all of the above processes, the organization of the chromophores is considered to be ideal for energy or electron transfer. Each chromophore is fixed at a distance and orientation that conserves the electronic interaction but avoids unnecessary quenching of the excited state. The exquisite organization of the chromophores is essential to the photophysical processes of the natural photosynthetic systems and should be applied to artificial multi-porphyrin systems.

Phosphorus(v) porphyrins[20] have stable axial substituents at the central six-coordinated phosphorus. Substitution of the axial ligands offers a synthetically simple and versatile means of modifying the porphyrin.[21–24] Also, the axial substituents can serve as bridges to other phosphorus(v) porphyrins. This prevents unnecessary quenching processes caused by significant π–π stacking of the porphyrin rings. Such simple structural modifications are key to the development of photosynthetic models. With this in mind, we have synthesized various types of phosphorus(v) porphyrin arrays.[21,22] In this study, "center-to-edge" type porphyrin dimers and trimers, in which the phenoxy group(s) at the *meso*-position of the phosphorus(v) porphyrin(s) are connected to the central phosphorus atom of the other phosphorus(v) porphyrin, are investigated. The axial phenoxy bridges hold the adjacent porphyrin rings in close proximity without causing a significant overlap of the porphyrin π systems. Such an arrangement of the "center-to-edge" type porphyrin arrays has some similarity to the geometry of the special pair in which two bacteriochlorophyll molecules are juxtaposed with only one pyrrole ring overlapping. Recently, various types of porphyrin arrays have been synthesized by axial coordination and structurally characterized.[8,10,11,13,14] However, the photophysical properties of these systems have not been fully investigated. Detailed investigation of the absorption and fluorescence properties of the present porphyrin arrays reveals the connection between structure and electronic coupling. In addition, this study points to a significant contribution of charge transfer character in the excited states. The importance of this phenomenon will be discussed in a comparison of the relaxation processes of two different types of phosphorus(v) porphyrin arrays, namely "center-to-edge" type and face-to-face type.

Results and discussion

Synthetic and structural aspects of "center-to-edge" type porphyrin arrays

The synthetic routes used to prepare the desired "center-to-edge" type phosphorus(v) porphyrin arrays are given in Scheme 1. The two chloride ligands of dichloro phosphorus(v) porphyrin are easily converted to various alkoxy or phenoxy ligands.[20f–h] Such synthetic versatility enables the fabrication of diverse multi-porphyrin systems.[21–24] We utilized 5-(4-hydroxyphenyl)-10,15,20-triphenylporphyrin as an axial ligand for the central phosphorus(v) porphyrin unit. After ligating to the central phosphorus(v) porphyrin through the phenoxy bridge, it is possible in both **H_2-P** and **H_2-P-H_2** to metallate the free-base outer porphyrin(s) with phosphorus atom(s). This repetitive cycle of axial ligand binding and subsequent metallation is a simple and versatile method for construction of supramolecular systems comprised of the phosphorus(v) porphyrins. All the synthetic porphyrin arrays were characterized by UV-vis, ^{1}H NMR, ^{31}P NMR and FAB mass spectra.

The proton-decoupled ^{31}P NMR spectra were used to con-

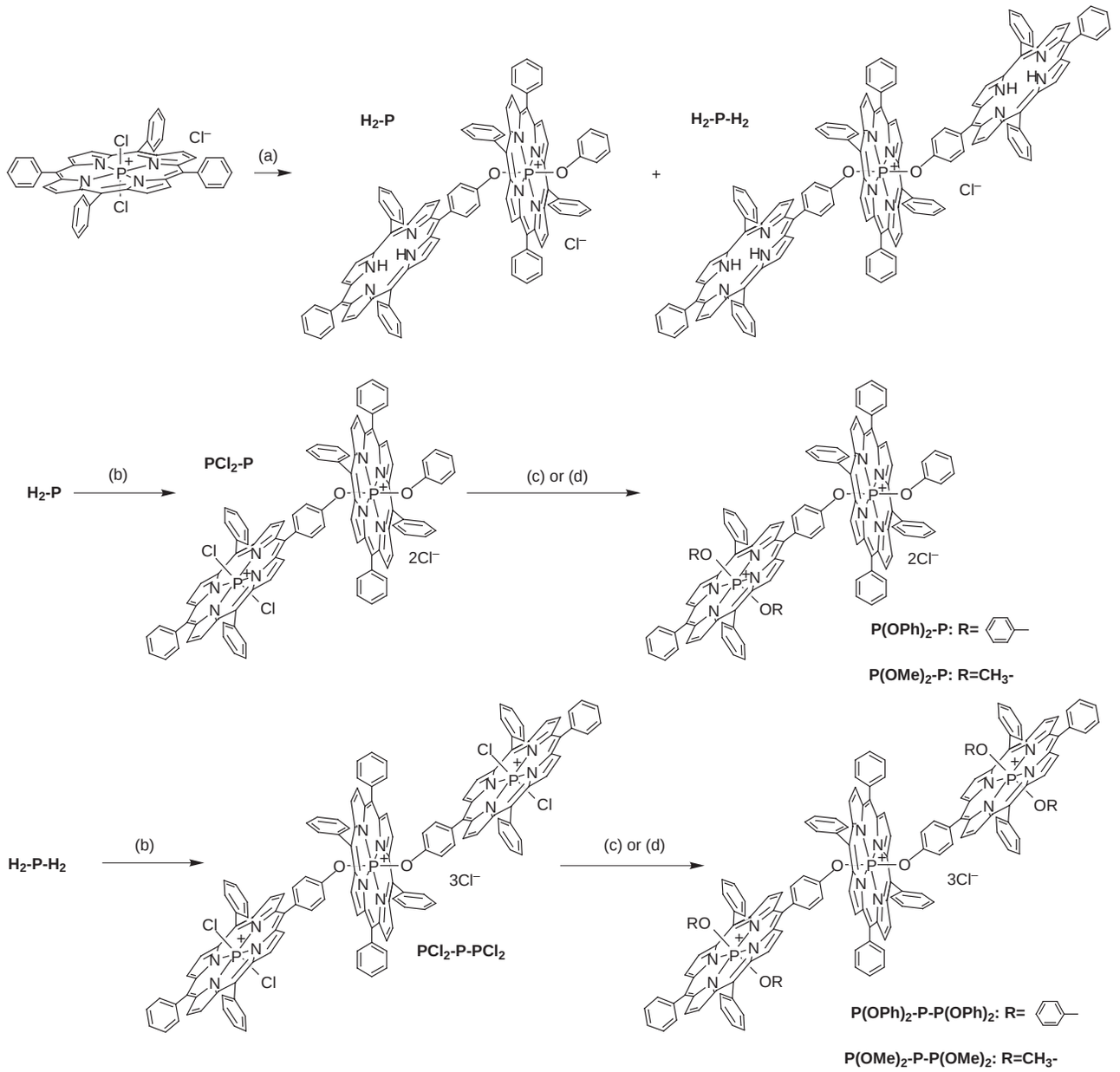

Scheme 1 *Reagents and conditions*: (a) 5-(4-hydroxyphenyl)-10,15,20-triphenylporphyrin, phenol, pyridine, reflux; (b) $POCl_3$, pyridine, reflux; (c) phenol, pyridine or CH_3CN, reflux; (d) methanol, reflux.

firm the axial coordination of the "center-to-edge" type phosphorus(v) porphyrin arrays. The proton-decoupled ^{31}P NMR spectra of the reference monomers gave singlet peaks at −229.2 ppm for **PCl_2**, −194.7 ppm for **$P(OPh)_2$** and −178.1 ppm for **$P(OMe)_2$**, respectively. These signals are in the typical range of hexacoordinated phosphorus compounds.[25] The "center-to-edge" type phosphorus(v) porphyrin arrays also exhibited one or two singlet peaks ascribed to each reference monomer according to the axial ligands.

^1H NMR studies give some structural information concerning the "center-to-edge" type phosphorus(v) porphyrin arrays. The large porphyrin ring current effect[26] on adjacent porphyrin subunits is a predominant feature in the ^1H NMR spectra of these closely-coupled arrays. An analysis of the ring current effect on adjacent porphyrin ring(s) can be used to deduce structural information about these arrays. Chemical shift values of the axial substituents as well as the β-protons on the porphyrin arrays and also the reference monomers are indicated in Fig. 1. The chemical shift values for the phenoxy protons of the bridge(s) and β-protons of the outer porphyrin ring(s) were shifted upfield and were dependent on the distance from the central porphyrin ring. The protons of the axial ligands on the outer porphyrin(s) were also shifted upfield relative to the reference monomers. These observations indicate that the outer porphyrin ring(s) are held within the shielding region of the central porphyrin ring. The β-protons of the central porphyrin ring in these arrays were shifted downfield relative to the reference monomer **$P(OPh)_2$** and depended on the number of ligated outer porphyrin rings. The protons on the independent (not bridging) phenoxy group which is ligated to the central porphyrin in the dimers (**PCl_2-P**, **$P(OPh)_2$-P** and **$P(OMe)_2$-P**) exhibit slight downfield shifts relative to those of **$P(OPh)_2$**. The downfield shift suggests that the axial phenoxy group on the central porphyrin lies in the deshielding region of the outer porphyrin ring of the opposite side. These results indicate that the conformation between the adjacent porphyrin rings is nearly vertical.

Absorption properties in CH_2Cl_2

The absorption data of the "center-to-edge" type phosphorus(v) porphyrin arrays and the reference monomers are summarized in Table 1. The absorption spectra of the mono-

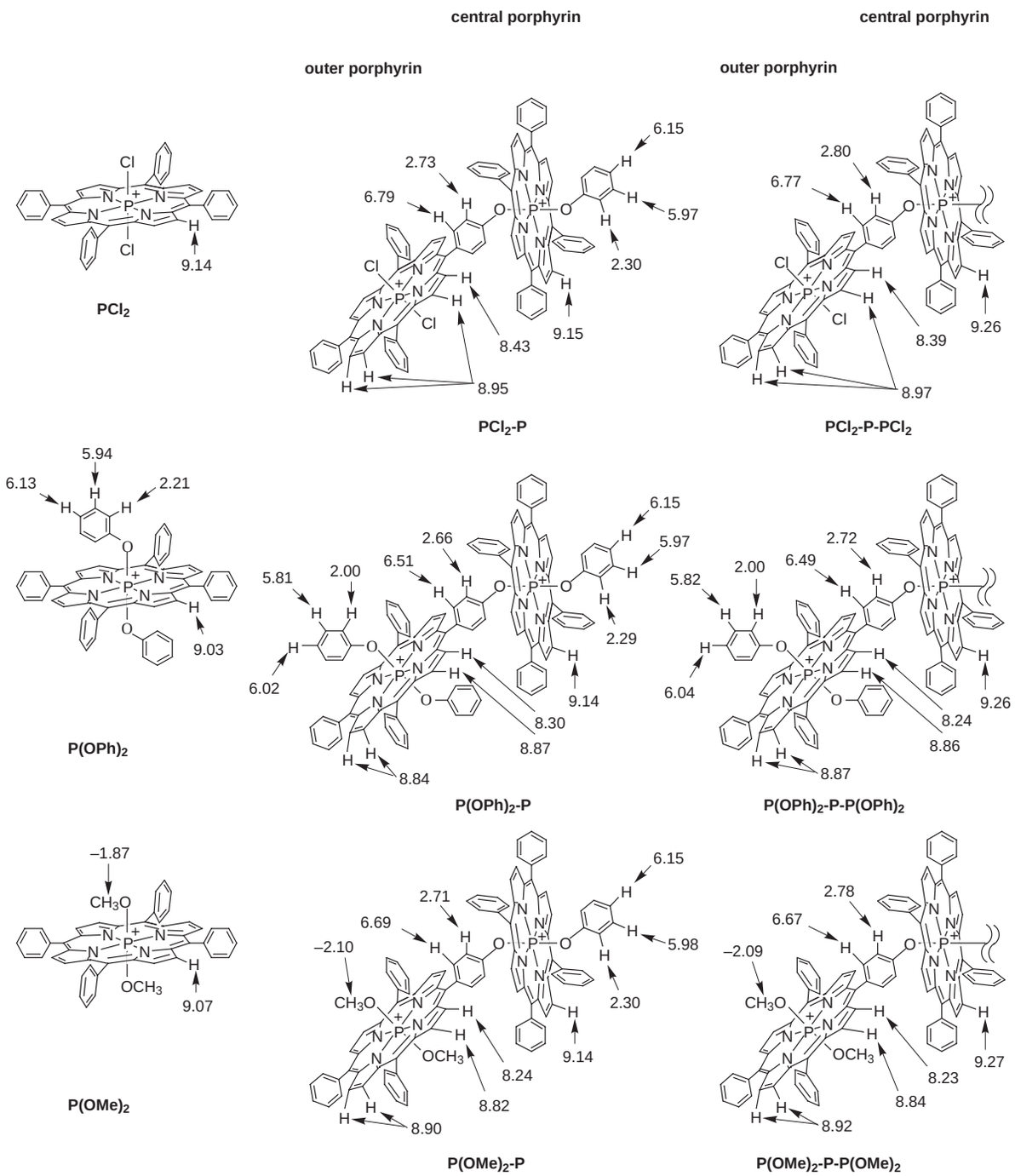

Fig. 1 Structures of the present porphyrin arrays and reference monomers. Chemical shifts of selected protons are also indicated.

mers (**PCl_2**, **$P(OPh)_2$** and **$P(OMe)_2$**) in CH_2Cl_2, are shown in Fig. 2. The intensity of the Soret band in **$P(OPh)_2$** is slightly diminished and the full width at half maximum (FWHM) of the Soret band in **$P(OPh)_2$** is broadened as compared with those of **PCl_2** and **$P(OMe)_2$**. The observed broadening in the absorption spectrum of **$P(OPh)_2$** suggests an electronic interaction between the axial phenoxy ligands and the porphyrin ring through the P–O bonds in the ground state of **$P(OPh)_2$**. This interaction through the axial phenoxy ligands may also induce the through-bond electronic communication between the porphyrin subunits in the "center-to-edge" type phosphorus(v) porphyrin arrays, whose axial phenoxy ligands are used as a bridge to link other phosphorus(v) porphyrin subunit(s). In fact, the absorption spectra of the phosphorus(v) porphyrin arrays are perturbed relative to the corresponding monomers. The intensities of the Soret bands in these arrays are markedly diminished relative to the simulated superimposed spectra of the corresponding monomers (Fig. 3). FWHMs of the Soret bands in these arrays are slightly increased (~300 cm^{-1}) as compared with those of the simulated spectra. However, the absorption maxima of the Soret and Q bands of these arrays were only 1–2 nm red-shifted from the respective bands in the simulated spectra. Since the energy levels of the phosphorus(v) porphyrin subunits in the arrays are sufficiently close to be resonant, excitonic interaction[27] should predominate in the absorption profile, especially for the Soret band. However, the slight shifts in the Soret regions of these arrays with respect to the reference monomers are suggestive of a weak excitonic interaction between the porphyrin subunits. This can be explained by the long center-to-center separation distance (*ca.* 10.0 Å)† and inappropriate orientation between the adjacent porphyrin rings. In the case of the Q bands, it is even more probable that the

† The center-to-center separated distance is estimated from a molecular space-filling model.

Table 1 Absorption properties of the porphyrin arrays and the reference monomers

Compound	Solvent	λ_{max}/nm [FWHM/cm^{-1}] Soret band	Q bands	
PCl_2	CH_2Cl_2	439 [710]	568 [780]	611 [550]
	(ε)[a]	(283000)	(12600)	(5950)
	acetone	437 [750]	567 [830]	611 [600]
	CH_3CN	436 [730]	566 [830]	609 [600]
$P(OPh)_2$	CH_2Cl_2	436 [1310]	562 [910]	605 [710]
	(ε)[a]	(184000)	(14100)	(4870)
	acetone	434 [1330]	561 [920]	603 [740]
	CH_3CN	433 [1290]	561 [920]	602 [780]
$P(OMe)_2$	CH_2Cl_2	430 [870]	560 [860]	601 [660]
	(ε)[a]	(327000)	(15800)	(3890)
	acetone	428 [860]	559 [850]	600 [660]
	CH_3CN	427 [860]	558 [860]	599 [720]
PCl_2-P	CH_2Cl_2	439 [1340]	566 [940]	612 [670]
	(ε)[a]	(316000)	(23300)	(10800)
	acetone	438 [1400]	566 [960]	612 [690]
	CH_3CN	437 [1360]	565 [950]	610 [690]
$P(OPh)_2$-P	CH_2Cl_2	436 [1590]	563 [950]	606 [780]
	(ε)[a]	(260000)	(23200)	(9370)
	acetone	435 [1630]	563 [960]	606 [790]
	CH_3CN	434 [1600]	562 [950]	605 [810]
$P(OMe)_2$-P	CH_2Cl_2	432 [1320]	562 [920]	604 [780]
	(ε)[a]	(293000)	(21700)	(7170)
	acetone	430 [1360]	561 [920]	603 [750]
	CH_3CN	429 [1360]	560 [910]	602 [770]
PCl_2-P-PCl_2	CH_2Cl_2	441 [1310]	568 [900]	614 [650]
	(ε)[a]	(359000)	(26200)	(13800)
	acetone	439 [1470]	567 [960]	612 [690]
	CH_3CN	437 [1410]	566 [940]	612 [660]
$P(OPh)_2$-P-$P(OPh)_2$	CH_2Cl_2	437 [1780]	564 [960]	608 [770]
	(ε)[a]	(341000)	(31000)	(13000)
	acetone	435 [1750]	563 [980]	606 [800]
	CH_3CN	434 [1710]	562 [960]	605 [780]
$P(OMe)_2$-P-$P(OMe)_2$	CH_2Cl_2	431 [1310]	562 [950]	605 [740]
	(ε)[a]	(406000)	(28200)	(9090)
	acetone	429 [1360]	561 [920]	604 [780]
	CH_3CN	428 [1350]	561 [920]	602 [770]

[a] Molar extinction coefficient (M^{-1} cm^{-1}) in CH_2Cl_2.

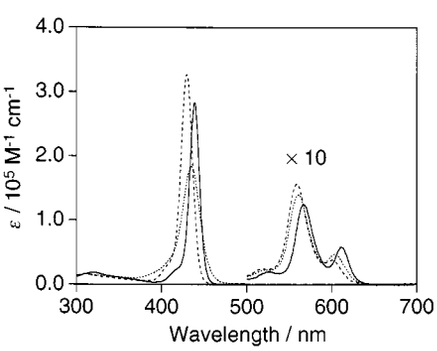

Fig. 2 Absorption spectra recorded in CH_2Cl_2 for **PCl_2** (solid line), **$P(OPh)_2$** (dotted line) and **$P(OMe)_2$** (dashed line).

contribution of exciton coupling between the adjacent porphyrin rings is quite small due to the fact that exciton coupling energy is proportional to the square of the transition dipole moments.

For better understanding of such interactions, the exciton coupling energy (V), which is the interaction energy due to exchange of excitation energy between molecules i and j, is often evaluated in the point-dipole approximation (eqn. (1)).[2–4,9,12] In this equation, e is the electronic charge and M_i is

$$V = (e^2 M_i M_j / R^3) F \qquad (1)$$

the monomer transition dipole length, R is a center-to-center separation distance and F is a geometrical factor. M_i can be

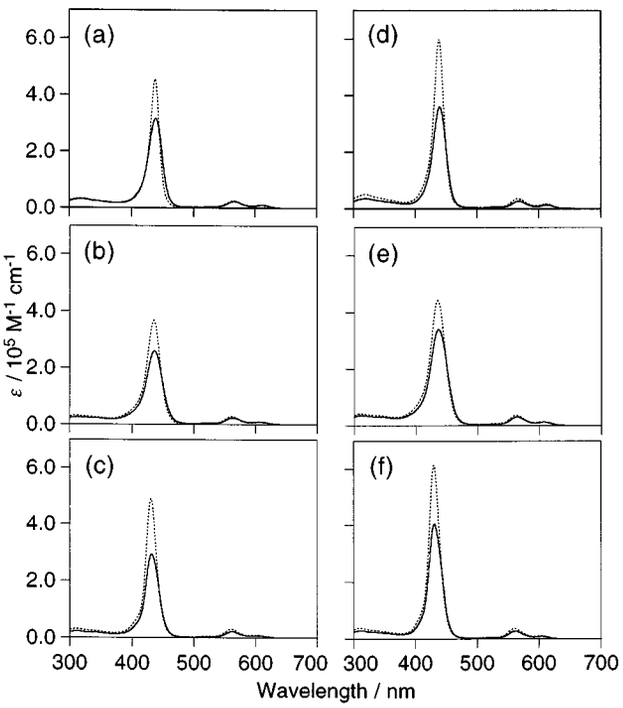

Fig. 3 Measured (solid line) and simulated (dotted line) absorption spectra recorded in CH_2Cl_2: (a) **PCl_2-P**; (b) **$P(OPh)_2$-P**; (c) **$P(OMe)_2$-P**; (d) **PCl_2-P-PCl_2**; (e) **$P(OPh)_2$-P-$P(OPh)_2$**; (f) **$P(OMe)_2$-P-$P(OMe)_2$**. Each simulated absorption spectrum is the superposition of the spectra of the reference monomers.

correlated to experimental absorption data by eqn. (2) where $\bar{\nu}$

$$(M_i)^2 = \frac{\varepsilon_{max}}{2500G} \times \frac{\Delta\bar{\nu}}{\nu} \qquad (2)$$

and ε_{max} are the transition energy and the molar extinction coefficient at the maximum of the considered absorption band, respectively, $\Delta\bar{\nu}$ is its full width at half maximum and G is the degeneracy. We applied such a treatment to **$P(OPh)_2$-P** which is a dimer comprised of essentially the same two monomer subunits (**$P(OPh)_2$**). The transition dipole lengths for the Soret (B) and Q bands are calculated from eqn. (2) and the spectral data for **$P(OPh)_2$**, and the values are $M_B^2 = 2.094$ Å^2 and $M_Q^2 = 0.143$ Å^2. Assuming that the center-to-center separation distance (the distance between the phosphorus nuclei) is 10.0 Å and F is equal to $(2/3)^{0.5}$ for a random distribution, calculated values of the exciton coupling energy (V_B and V_Q) are 199 cm^{-1} and 14 cm^{-1}, respectively. The exciton coupling energies of **$P(OPh)_2$-P** are small as compared with those of other face-to-face porphyrin dimers.[2,3,9,12] Even if the geometry between the porphyrin rings was optimal for excitonic interaction, the exciton coupling energy of this system would still be small. The slight shift in the Soret region of **$P(OPh)_2$-P** relative to **$P(OPh)_2$** reflects the small V_B. For the Q bands, the exciton coupling effect is too small and disappears in the inhomogeneous solvent broadening. So it is reasonable to conclude that the slight red shifts of the Q bands are induced from the solvation difference[28] of the monomer and the dimer rather than the exciton coupling effect. These lines are expected to be similar to the absorption profiles of the other "center-to-edge" type phosphorus(v) porphyrin arrays. The observed absorption properties of the arrays suggest that the π systems of the individual porphyrin rings are weakly coupled through the axial bond.

Fluorescence properties in CH_2Cl_2

Fluorescence properties in CH_2Cl_2 were investigated to confirm the above electronic interaction between the porphyrin rings in the excited states of these arrays. As shown in Table 2, the (0,0)

Table 2 Fluorescence properties of the porphyrin arrays and the reference monomers

Compound	Solvent	λ_{max}/nm	Stokes shift/ cm^{-1}	$E(S_1)$/ eV
PCl_2	CH_2Cl_2	624, 679	341	2.01
	acetone	624, 678	341	2.01
	CH_3CN	622, 677	343	2.01
$P(OPh)_2$	CH_2Cl_2	623, 674	478	2.02
	acetone	622, 674	507	2.02
	CH_3CN	622, 672	534	2.03
$P(OMe)_2$	CH_2Cl_2	619, 671	484	2.03
	acetone	617, 670	459	2.04
	CH_3CN	617, 669	487	2.04
PCl_2-P	CH_2Cl_2	629, 681	442	2.00
	acetone	629, 680	442	2.00
	CH_3CN	628, 680	470	2.00
$P(OPh)_2$-P	CH_2Cl_2	626, 677	527	2.01
	acetone	626, 676	527	2.01
	CH_3CN	625, 675	529	2.02
$P(OMe)_2$-P	CH_2Cl_2	623, 675	505	2.02
	acetone	622, 672	507	2.02
	CH_3CN	622, 672	534	2.03
PCl_2-P-PCl_2	CH_2Cl_2	629, 683	388	2.00
	acetone	630, 681	467	2.00
	CH_3CN	627, 679	391	2.00
$P(OPh)_2$-P-$P(OPh)_2$	CH_2Cl_2	628, 678	524	2.01
	acetone	626, 676	527	2.01
	CH_3CN	625, 676	529	2.02
$P(OMe)_2$-P-$P(OMe)_2$	CH_2Cl_2	624, 676	503	2.02
	acetone	621, 672	453	2.02
	CH_3CN	621, 673	508	2.03

fluorescence bands of these arrays were slightly red-shifted from those of the corresponding monomers and we can see similar trends in the absorption spectra, indicating weakly coupled π systems. Furthermore, the similarity in the Stokes shifts for these arrays and their corresponding monomers indicates that the nuclear displacements in the excited states of these arrays are small.

On the other hand, the fluorescence quantum yields and lifetimes of the arrays in CH_2Cl_2 changed, albeit slightly, even though the interaction in the ground state between the porphyrin rings was small (Table 3). Fluorescence lifetime measurements were made using the time-correlated single photon counting method and each of the obtained decay curves exhibited a single-exponential fitting. In CH_2Cl_2 the fluorescence quantum yields and the fluorescence lifetimes for **PCl_2-P** and **PCl_2-P-PCl_2** were smaller than those of **$P(OPh)_2$** but similar to those of **PCl_2**, suggesting that the lowest excited state is localized on a **PCl_2** subunit and the intersystem crossing induced by the heavy atom effect of the axial chloride ligands dominates the decay process for **PCl_2-P** and **PCl_2-P-PCl_2**. The fluorescence quantum yields and the fluorescence lifetimes for **$P(OPh)_2$-P**, **$P(OPh)_2$-P-$P(OPh)_2$**, **$P(OMe)_2$-P** and **$P(OMe)_2$-P-$P(OMe)_2$** in CH_2Cl_2 were reduced relative to the corresponding monomers, although the degree of the quenching is not significant. Such fluorescence quenching is found for other porphyrin arrays as well[3,5,9a] and is often explained as an enhancement of the nonradiative decay processes due to exciton coupling and/or charge transfer interaction.‡ The exciton coupling within the porphyrin arrays gives rise to splitting of the energy levels of the excited

‡ Intersystem crossing should be also considered as one of the possibilities to enhance the fluorescence quenching. However, our preliminary results of time-resolved EPR showed similar zero-field splitting parameters between phosphorus(V) porphyrin monomers and phosphorus(V) porphyrin arrays, indicating that probabilities of intersystem crossing of the phosphorus(V) porphyrin arrays are almost the same as those of the corresponding monomers and spin-orbit coupling does not contribute to the enhancement of nonradiative decay of the arrays as compared with that of the corresponding monomers.

Table 3 Fluorescence quantum yields and lifetimes for the porphyrin arrays and the reference monomers

Compound	Solvent	Φ_f	τ_f/ns
PCl_2	CH_2Cl_2	0.011	0.82
	acetone	0.010	0.84
	CH_3CN	0.010	0.91
$P(OPh)_2$	CH_2Cl_2	0.037	2.92
	acetone	0.014	1.47
	CH_3CN	0.016	1.62
$P(OMe)_2$	CH_2Cl_2	0.044	3.87
	acetone	0.047	5.13
	CH_3CN	0.044	4.48
PCl_2-P	CH_2Cl_2	0.012	0.84
	acetone	0.0087	0.56
	CH_3CN	0.0059	0.49
$P(OPh)_2$-P	CH_2Cl_2	0.025	1.55
	acetone	0.0094	0.70
	CH_3CN	0.0073	0.65
$P(OMe)_2$-P	CH_2Cl_2	0.022	1.51
	acetone	0.0058	0.52
	CH_3CN	0.0041	0.42
PCl_2-P-PCl_2	CH_2Cl_2	0.010	0.67
	acetone	0.0069	0.49
	CH_3CN	0.0067	0.51
$P(OPh)_2$-P-$P(OPh)_2$	CH_2Cl_2	0.010	0.76
	acetone	0.0040	0.36
	CH_3CN	0.0039	0.36
$P(OMe)_2$-P-$P(OMe)_2$	CH_2Cl_2	0.0080	0.74
	acetone	0.0021	0.23
	CH_3CN	0.0019	0.21

states. This exciton splitting reduces the energy gap between the ground and excited states and thus increases the chance to couple them to each other.[6,9a] However, the present small exciton coupling effect of the arrays would contribute very little to the fluorescence quenching. On the other hand, if the fluorescence quenching is enhanced with increasing solvent polarity, the contribution of the charge transfer interaction should be taken into account as a possible decay process.[6,7,9a,21b] These points will be further discussed below.

Solvent-polarity dependent photophysics of the porphyrin arrays

The extent to which the excited charge transfer interaction contributes to the decay process of the porphyrin arrays can be examined by the solvent-polarity dependent fluorescence properties. An increase in solvent polarity should increase the charge transfer interaction resulting in a greater degree of fluorescence quenching.

The absorption properties of the "center-to-edge" type phosphorus(V) porphyrin arrays and the reference monomers were independent of solvent polarity (Table 1). The energy levels of the lowest excited singlet states and Stokes shifts for these arrays were also essentially independent of solvent polarity (Table 2). Thus, the Franck–Condon factor between the lowest excited singlet state and the ground state is not significantly perturbed by a difference in solvent polarity. However, an obvious decrease of the fluorescence quantum yields and the shortening of the fluorescence lifetimes for these arrays compared with those for the reference monomers were observed with increasing solvent polarity (Table 3). These results can be ascribed to an enhancement of a nonradiative decay rather than a radiative decay.§ The presence of the new decay channel in polar solvents suggests that the contribution of the charge transfer to the nonradiative decay of the excited singlet state is enhanced and the nonradiative decay rate is accelerated. **$P(OPh)_2$** also exhibited a slight enhancement of the nonradiative decay dependent on solvent polarity. Recently, the

§ The radiative and nonradiative decay rate constants (k_r and k_{nr}) were calculated by $k_r = \Phi_f/\tau_f$, $k_{nr} = (1 - \Phi_f)/\tau_f$ where Φ_f and τ_f are the fluorescence quantum yield and the lifetime, respectively.

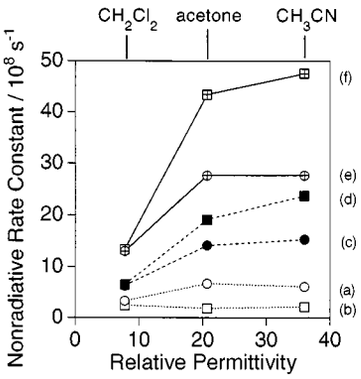

Fig. 4 Dependence of nonradiative decay rate constants on solvent relative permittivity: (a) **P(OPh)$_2$**; (b) **P(OMe)$_2$**; (c) **P(OPh)$_2$-P**; (d) **P(OMe)$_2$-P**; (e) **P(OPh)$_2$-P-P(OPh)$_2$**; (f) **P(OMe)$_2$-P-P(OMe)$_2$**.

photophysical properties of the phosphorus(v) porphyrins with various phenoxy ligands were reported.[20m] The solvent polarity dependent photophysics indicated that charge transfer from the axial phenoxy ligands to the phosphorus(v) porphyrin ring participated in the deactivation processes of the excited states of a series of diaryloxy phosphorus(v) porphyrins. Also the contribution of the charge transfer character was proportional to the electron-donating ability of the substituents of the axial phenoxy ligands. The application of these data to the photophysics of the present phosphorus(v) porphyrin arrays predicts a reduction in the charge transfer from the axial phenoxy ligands to the phosphorus(v) porphyrin because the outer phosphorus(v) porphyrin rings are expected to act as electron-withdrawing substituents toward the axial phenoxy ligand. However, the enhancement of the nonradiative decay processes in these arrays are larger than that of **P(OPh)$_2$** as the solvent polarity increases. Furthermore, as shown in Fig. 4, the nonradiative decay processes of **P(OMe)$_2$-P** and **P(OMe)$_2$-P-P(OMe)$_2$**, which are comprised of different subunits (**P(OPh)$_2$** and **P(OMe)$_2$**), are more sensitive to solvent polarity than those of **P(OPh)$_2$-P** and **P(OPh)$_2$-P-P(OPh)$_2$**, which are comprised of the same subunits (**P(OPh)$_2$**). Since the redox properties of **P(OPh)$_2$** and **P(OMe)$_2$** are different, it is reasonable to consider that the energy levels of the charge transfer states of **P(OMe)$_2$-P** and **P(OMe)$_2$-P-P(OMe)$_2$** are more stabilized than those of **P(OPh)$_2$-P** and **P(OPh)$_2$-P-P(OPh)$_2$**, respectively.¶ This leads to the conclusion that the enhancement of the solvent-polarity dependent nonradiative decay processes is ascribed to the contribution of the charge transfer interaction between the phosphorus(v) porphyrins. Also, we note that the contribution of the charge transfer state can enhance nonradiative transitions from the excited singlet state even if the energy level of the charge transfer state is higher than that of the lowest excited singlet state.[7,9a,21b]

In symmetric bichromophoric molecules, the coupling of the two charge transfer configurations with each other keeps the electronic symmetry equilibrated. However, symmetry reduction can be induced by interaction between the charge transfer

¶ Reduction potentials of the phosphorus(v) porphyrin derivatives were determined in CH_2Cl_2 containing 0.1 M n-Bu_4NClO_4 using platinum working and counter electrodes and a saturated calomel reference electrode. **PCl$_2$**: $E_{red} = -0.28$ V; **P(OPh)$_2$**: $E_{red} = -0.44$ V; **P(OMe)$_2$**: $E_{red} = -0.50$ V; **PCl$_2$-P**: $E_{red} = -0.24$, -0.42 V; **P(OPh)$_2$-P**: $E_{red} = -0.41$ V; **P(OMe)$_2$-P**: $E_{red} = -0.38$, -0.52 V; **PCl$_2$-P-PCl$_2$**: $E_{red} = -0.23$, -0.39 V; **P(OPh)$_2$-P-P(OPh)$_2$**: $E_{red} = -0.32$, -0.45 V; **P(OMe)$_2$-P-P(OMe)$_2$**: $E_{red} = -0.37$, -0.51 V. Each E_{red} value of the dimers and trimers is nearly the same as those of the corresponding monomer units although the interaction between the porphyrin rings causes a small shift of the reduction potentials. On the other hand, the oxidation of phosphorus(v) porphyrin ring yielded irreversible cyclic voltammograms. This unfavorable result prevented us from estimating the accurate energy levels of the charge transfer states.

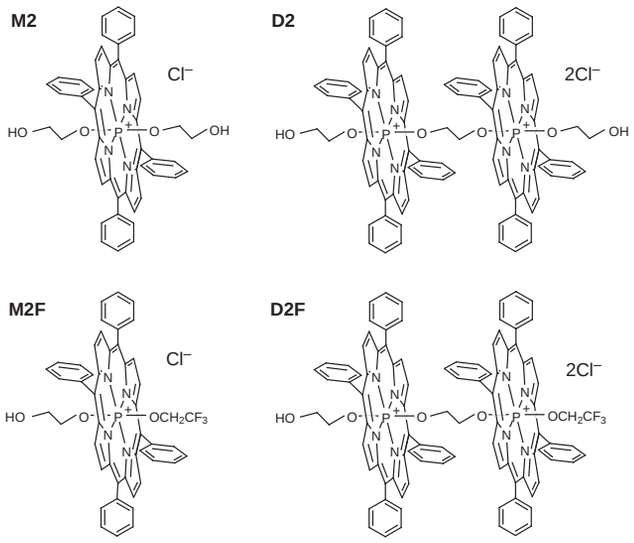

Fig. 5 Structures of the "wheel-and-axle" type phosphorus(v) porphyrin arrays and reference monomers. For other porphyrin arrays with similar structure, see ref. 21.

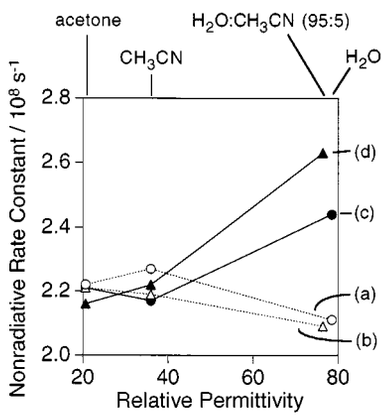

Fig. 6 Dependence of nonradiative decay rate constants of "wheel-and-axle" type phosphorus(v) porphyrin arrays and reference monomers on solvent relative permittivity: (a) **M2**; (b) **M2F**; (c) **D2**; (d) **D2F**. For **M2F** and **D2F**, the relative permittivity of H_2O–CH_3CN (95 : 5) was assumed to be 76.4 (from ref. 21(*b*)).

configuration and the fluctuating unsymmetrical solvent environment.[29] The perturbation induced by solvent fluctuation brings about the decoupling of the two charge transfer configurations and the charge transfer state is stabilized by the solvation of the charges as the solvent polarity increases. Due to the stabilization of the charge transfer state, it is possible that nonradiative transitions between the lowest excited singlet states and the ground states in these arrays are enhanced by the charge transfer state. Furthermore, the symmetry-disturbed systems have nonzero ground state dipole moments which lead to a gradient in the excited state towards the more stabilized charge transfer state and induce presolvation in the ground states in contrast to the symmetric systems.[30] This situation favors the formation of the charge transfer state. The enhancement of nonradiative decay by an increase in charge transfer character is reported in other multi-porphyrin systems.[6,7,9a,21b]

Recently, we have discussed the charge transfer character in the excited states of the "wheel-and-axle" type phosphorus(v) porphyrin arrays, whose central phosphorus atoms are connected to each other by various lengths of the alkyldioxy bridge (Fig. 5).[21b,22a] These face-to-face type phosphorus(v) porphyrin arrays also exhibit similar fluorescence quenching processes with partially stacked geometry induced by a polar environment. Solvent polarity dependence of nonradiative rate constants for the face-to-face type porphyrin arrays are also shown in Fig. 6.[21b] Comparison of the solvent-polarity dependent

photophysics between the "center-to-edge" type arrays and the face-to-face type arrays (Figs. 4 and 6) suggests that the contribution of the excited charge transfer state to the nonradiative decay process is greater in the former, more so than the latter. The contribution of the excited charge transfer state in the "center-to-edge" type porphyrin arrays is much more significant even in medium polar solvents relative to that in the face-to-face type porphyrin arrays. For the face-to-face type porphyrin arrays, the contribution of the excited charge transfer state can be seen only in a highly polar solvent (H_2O–CH_3CN (95 : 5) and H_2O) and is very small. These results suggest that the relaxation processes of the excited states of the phosphorus(v) porphyrin arrays are tunable by not only environmental factors (solvent) but also the geometry and connectivity between the porphyrin rings. In addition, it is interesting that the "center-to-edge" type porphyrin arrays, which have small overlapped geometry between the porphyrin rings, showed a larger contribution of charge transfer character than the face-to-face type porphyrin arrays, which have maximum overlap of their π systems. This trend is reminiscent of the "minimum overlap rule",[29] which implies that the degree of charge separation is maximized for perpendicularly twisted π systems. This principle also holds for small overlapped π systems which are not strictly orthogonal but are separated in space. The consideration along this line may be useful to understand the structural relationship to the photophysical properties of phosphorus(v) porphyrin arrays and gives us further insight to design more sophisticated photosynthetic models.

Conclusion

The repetitive cycles of phosphorus atom insertion and subsequent axial substitution have enabled the construction of "center-to-edge" type phosphorus(v) porphyrin arrays. The axial phenoxy bridges in these arrays hold the adjacent porphyrin rings in close proximity while avoiding a significant overlap of their π-systems. This prevents unnecessary quenching due to π–π stacking of the porphyrin rings.

The absorption and fluorescence properties of the "center-to-edge" type phosphorus(v) porphyrin arrays in a nonpolar environment originally suggested only a small excitonic and electronic interaction between the porphyrin rings. However, solvent-polarity dependent photophysics of the "center-to-edge" type phosphorus(v) porphyrin arrays revealed the contribution of the excited charge transfer character to the nonradiative decay in polar environments. The amount by which the nonradiative decay rate constants are enhanced is significantly different for the two types of phosphorus(v) porphyrin arrays, the "center-to-edge" type and the face-to-face type. This suggests that the geometry and connectivity between the chromophores are key factors in controlling the decay processes of the excited states. The excited charge transfer character is considered to be responsible for the ultrafast and unidirectional electron transfer in the sequential charge separation processes carried out in the reaction center and has been suggested from both an experimental[31] and a theoretical[32] perspective. The similar charge transfer character of the phosphorus(v) porphyrin arrays gives us an insight into understanding the factors that govern the efficient electron transfer processes in natural photosynthetic systems.

Experimental

Measurements

^{1}H and ^{31}P NMR spectra were recorded on a JEOL EX-270KS (400 MHz) spectrometer and a JEOL EX-90 spectrometer, respectively. Chemical shifts of ^{1}H and ^{31}P are reported in δ units relative to tetramethylsilane (TMS) internal standard for ^{1}H and 85% H_3PO_4 external standard for ^{31}P, respectively.

Absorption spectra were recorded on a Shimadzu UV-2200 spectrophotometer. Fluorescence spectra were recorded on a Shimadzu RF-503A spectrofluorimeter.

Time-resolved fluorescence spectra were measured by the two-dimensional photon-counting technique using a streak-camera (Hamamatsu, C4334 streakscope, time resolution: *ca.* 15 ps) and an excitation pulse source of a mode-locked Ti–sapphire laser (Spectra Physics, Tsunami, frequency-doubled excitation pulse: 400 nm, 200 fs). A glass cut-off filter was used to isolate fluorescence from scattered laser light. Excited singlet state lifetimes were determined by the computer deconvolution analysis of the spectra to minimize their chi-square parameters.

All the samples were purified again by column chromatography and the homogeneity of each sample was checked by thin layer chromatography prior to use.

Materials

The porphyrin derivatives used in this study are given in Scheme 1 or Fig. 1. The phosphorus(v) tetraphenylporphyrin monomer derivatives **PCl_2**, **$P(OPh)_2$** and **$P(OMe)_2$** were prepared as described previously.[20d,f] Heterodimer **H_2-P** and heterotrimer **H_2-P-H_2** (Scheme 1) were also prepared as described previously.[22]

PCl_2-P. H_2-P (0.1123 g, 8.01×10^{-5} mol) and phosphorus oxychloride (1.50 ml, 1.61×10^{-2} mol) were dissolved and refluxed in 10 ml of dry pyridine under nitrogen. The reaction mixture was stirred and monitored by thin layer chromatography in $CHCl_3$–MeOH (5 : 1), and a further 4.0 ml of dry pyridine and 2.0 ml of phosphorus oxychloride were added in the course of this reaction. After 9 days, the solvent and excess $POCl_3$ were removed *in vacuo*. The residues were separated by column chromatography on silica gel with $CHCl_3$–MeOH (5 : 1) to yield 0.0925 g (75%) of the product. UV-vis (CH_2Cl_2): λ_{max} 439, 566, 612 nm. ^{1}H NMR (400 MHz, $CDCl_3$): δ 2.30 (d, 2H, phenyl-H), 2.73 (d, 2H, phenyl-H), 5.97 (t, 2H, phenyl-H), 6.15 (t, 1H, phenyl-H), 6.79 (d, 2H, phenyl-H), 7.67–7.80 (m, 21H, phenyl-H), 7.84–7.97 (m, 14H, phenyl-H), 8.43 (dd, 2H, β-H), 8.95 (m, 6H, β-H), 9.15 (d, 8H, β-H). ^{31}P NMR (90 MHz, $CDCl_3$): δ −229.2 (s, outer dichloro P(v) porphyrin subunit), −195.3 (s, central diphenoxy P(v) porphyrin subunit). FAB HRMS: *m*/*z*: 1464.376 (M^+). Calculated for $C_{94}H_{60}N_8O_2P_2Cl_2$, 1464.3692.

$P(OPh)_2$-P. PCl_2-P (0.0202 g, 1.31×10^{-5} mol) and phenol (0.1594 g, 1.69×10^{-3} mol) were dissolved and refluxed in 3 ml of dry pyridine. After 2 days, the solvent was removed *in vacuo*. The residue was separated by column chromatography on silica gel with $CHCl_3$–MeOH (5 : 1) to yield 0.0104 g (48%) of the product. UV-vis (CH_2Cl_2): λ_{max} 436, 563, 606 nm. ^{1}H NMR (400 MHz, $CDCl_3$): δ 2.00 (d, 4H, phenyl-H), 2.29 (d, 2H, phenyl-H), 2.66 (d, 2H, phenyl-H), 5.81 (t, 4H, phenyl-H), 5.97 (t, 2H, phenyl-H), 6.02 (t, 2H, phenyl-H), 6.15 (t, 1H, phenyl-H), 6.51 (d, 2H, phenyl-H), 7.61–7.78 (m, 27H, phenyl-H), 7.91 (m, 8H, phenyl-H), 8.30 (dd, 2H, β-H), 8.84 (d, 4H, β-H), 8.87 (dd, 2H, β-H), 9.14 (d, 8H, β-H). ^{31}P NMR (90 MHz, $CDCl_3$): δ −195.5 (s). FAB HRMS: *m*/*z*: 1580.506 (M^+). Calculated for $C_{106}H_{70}N_8O_4P_2$, 1580.4995.

$P(OMe)_2$-P. PCl_2-P (0.0273 g, 1.78×10^{-5} mol) was dissolved and refluxed in 4 ml of dry methanol. After 3 days, the solvent was removed *in vacuo*. The residue was separated by column chromatography on silica gel with $CHCl_3$–MeOH (5 : 1) to yield 0.017 g (62%) of the product. UV-vis (CH_2Cl_2): λ_{max} 432, 562, 604 nm. ^{1}H NMR (400 MHz, $CDCl_3$): δ −2.10 (d, 6H, -OCH_3), 2.30 (d, 2H, phenyl-H), 2.71 (d, 2H, phenyl-H), 5.98 (t, 2H, phenyl-H), 6.15 (t, 1H, phenyl-H), 6.69 (d, 2H, phenyl-H), 7.66–7.79 (m, 21H, phenyl-H), 7.83 (m, 6H, phenyl-H), 7.93 (m, 8H, phenyl-H), 8.24 (dd, 2H, β-H), 8.82 (dd, 2H, β-H), 8.90 (d,

4H, β-H), 9.14 (d, 8H, β-H). ^{31}P NMR (90 MHz, $CDCl_3$): δ −195.3 (s, central diphenoxy P(v) porphyrin subunit), −178.2 (s, outer dimethoxy P(v) porphyrin subunit). FAB HRMS: *m*/*z*: 1456.475 (M^+). Calculated for $C_{96}H_{66}N_8O_4P_2$, 1456.4682.

PCl_2-P-PCl_2. H_2-P-H_2 (0.082 g, 4.23×10^{-5} mol) and phosphorus oxychloride (0.50 ml, 5.36×10^{-3} mol) were dissolved and refluxed in 5 ml of dry pyridine under nitrogen. The reaction mixture was stirred under the supervision of thin layer chromatography in $CHCl_3$–MeOH (5:1), and 1 ml of dry pyridine and 3.5 ml of phosphorus oxychloride were added in the course of this reaction. After 10 days, the solvent and excess $POCl_3$ were removed *in vacuo*. The residues were separated by column chromatography on silica gel with $CHCl_3$–MeOH (5:1) to yield 0.0808 g (86%) of the product. UV-vis (CH_2Cl_2): λ_{max} 441, 568, 614 nm. ^{1}H NMR (400 MHz, $CDCl_3$): δ 2.80 (d, 4H, phenyl-H), 6.77 (d, 4H, phenyl-H), 7.67–7.81 (m, 30H, phenyl-H), 7.90 (m, 12H, phenyl-H), 8.08 (m, 8H, phenyl-H), 8.39 (dd, 4H, β-H), 8.97 (d, 8H, β-H), 8.97 (m, 4H, β-H), 9.26 (d, 8H, β-H). ^{31}P NMR (90 MHz, $CDCl_3$): δ −229.2 (s, outer dichloro P(v) porphyrin subunit), −195.8 (s, central diphenoxy P(v) porphyrin subunit). FAB HRMS: *m*/*z*: 2099.530 (M^+). Calculated for $C_{132}H_{82}N_{12}O_2P_3Cl_4$, 2099.4651.

$P(OPh)_2$-P-$P(OPh)_2$. PCl_2-P-PCl_2 (0.063 g, 2.85×10^{-5} mol) and phenol (1.035 g, 1.10×10^{-2} mol) were dissolved and refluxed in 3 ml of dry acetonitrile for 12 hours. After the solvent was removed *in vacuo*, the residues were separated by column chromatography on silica gel with $CHCl_3$–MeOH (5:1) to yield 0.052 g (75%) of the product. UV-vis (CH_2Cl_2): λ_{max} 437, 564, 608 nm. ^{1}H NMR (400 MHz, $CDCl_3$): δ 2.00 (d, 8H, phenyl-H), 2.72 (d, 4H, phenyl-H), 5.82 (t, 8H, phenyl-H), 6.04 (t, 4H, phenyl-H), 6.49 (d, 4H, phenyl-H), 7.6–7.8 (m, 42H, phenyl-H), 8.04 (m, 8H, phenyl-H), 8.24 (dd, 4H, β-H), 8.86 (m, 4H, β-H), 8.87 (d, 8H, β-H), 9.26 (d, 8H, β-H). ^{31}P NMR (90 MHz, $CDCl_3$): δ −195.8 (s, central diphenoxy P(v) porphyrin subunit), −195.3 (s, outer diphenoxy P(v) porphyrin subunit). FAB HRMS: *m*/*z*: 2331.715 (M^+). Calculated for $C_{156}H_{102}N_{12}O_6P_3$, 2331.7258.

$P(OMe)_2$-P-$P(OMe)_2$. PCl_2-P-PCl_2 (0.0209 g, 9.46×10^{-6} mol) was dissolved and refluxed in 5 ml of dry methanol for 61 hours. After the solvent was removed *in vacuo*, the residues were separated by column chromatography on silica gel with $CHCl_3$–MeOH (5:1) to yield 0.0170 g (82%) of the product. UV-vis (CH_2Cl_2): λ_{max} 432, 562, 604 nm. ^{1}H NMR (400 MHz, $CDCl_3$): δ −2.09 (d, 12H, -OCH_3), 2.78 (d, 4H, phenyl-H), 6.67 (d, 4H, phenyl-H), 7.68–7.80 (m, 30H, phenyl-H), 7.84 (m, 12H, phenyl-H), 8.08 (m, 8H, phenyl-H), 8.23 (dd, 4H, β-H), 8.84 (dd, 4H, β-H), 8.92 (d, 8H, β-H), 9.27 (d, 8H, β-H). ^{31}P NMR (90 MHz, $CDCl_3$): δ −195.7 (s, central diphenoxy P(v) porphyrin subunit), −178.2 (s, outer dimethoxy P(v) porphyrin subunit). FAB HRMS: *m*/*z*: 2083.648 (M^+). Calculated for $C_{136}H_{94}N_{12}O_6P_3$, 2083.6632.

Acknowledgements

The authors thank Dr K. Ishii and Professor S. Yamauchi at Tohoku University for the measurement and discussion of time-resolved EPR. This work was supported by grants from the Ministry of Education, Science, and Culture of the Japanese Government (Priority Area 282) and grants from "Field and Reaction", PRESTO, JST.

References

1 M. R. Wasielewski, *Chem. Rev.*, 1992, **92**, 435 and references cited therein.
2 M. Gouterman, D. Holten and E. Lieberman, *Chem. Phys.*, 1977, **25**, 139.
3 C. K. Chang, *J. Heterocycl. Chem.*, 1977, **14**, 1285.
4 R. Selensky, D. Holten, M. W. Windsor, J. B. Paine III, D. Dolphin, M. Gouterman and J. C. Thomas, *Chem. Phys.*, 1981, **60**, 33.
5 (*a*) A. Osuka, S. Nakajima, T. Nagata, K. Maruyama and K. Toriumi, *Angew. Chem., Int. Ed. Engl.*, 1991, **30**, 582; (*b*) A. Osuka, S. Nakajima and K. Maruyama, *J. Org. Chem.*, 1992, **57**, 7355; (*c*) A. Osuka, B. Liu and K. Maruyama, *J. Org. Chem.*, 1993, **58**, 3582.
6 J. L. Sessler, V. L. Capuano and A. Harriman, *J. Am. Chem. Soc.*, 1993, **115**, 4618.
7 (*a*) D. G. Johnson, W. A. Svec and M. R. Wasielewski, *Isr. J. Chem.*, 1988, **28**, 193; (*b*) S. G. Johnson, G. J. Small, D. G. Johnson, W. A. Svec and M. R. Wasielewski, *J. Phys. Chem.*, 1989, **93**, 5437; (*c*) M. R. Wasielewski, D. G. Johnson, M. P. Niemczyk, G. L. Gaines, III, M. P. O'Neil and W. A. Svec, *J. Am. Chem. Soc.*, 1990, **112**, 6482.
8 (*a*) X. Chi, A. J. Guerin, R. A. Haycock, C. A. Hunter and L. D. Sarson, *J. Chem. Soc., Chem. Commun.*, 1995, 2563; (*b*) X. Chi, A. J. Guerin, R. A. Haycock, C. A. Hunter and L. D. Sarson, *J. Chem. Soc., Chem. Commun.*, 1995, 2567.
9 (*a*) T. H. Tran-Thi, J. F. Lipskier, P. Maillard, M. Momenteau, J.-M. Lopez-Castillo and J.-P. Jay-Gerin, *J. Phys. Chem.*, 1992, **96**, 1073; (*b*) T. H. Tran-Thi, A. Dormond and R. Guilard, *J. Phys. Chem.*, 1992, **96**, 3139.
10 Y. Kobuke and H. Miyaji, *J. Am. Chem. Soc.*, 1994, **116**, 4111.
11 A. K. Burrell, D. L. Officer, D. C. W. Reid and K. Y. Wild, *Angew. Chem., Int. Ed.*, 1998, **37**, 114.
12 X. Yan and D. Holten, *J. Phys. Chem.*, 1988, **92**, 409.
13 (*a*) N. Kariya, T. Imamura and Y. Sasaki, *Inorg. Chem.*, 1997, **36**, 833; (*b*) K. Funatsu, A. Kimura, T. Imamura, A. Ichimura and Y. Sasaki, *Inorg. Chem.*, 1997, **36**, 1625; (*c*) N. Kariya, T. Imamura and Y. Sasaki, *Inorg. Chem.*, 1998, **37**, 1658; (*d*) K. Funatsu, T. Imamura, A. Ichimura and Y. Sasaki, *Inorg. Chem.*, 1998, **37**, 1798.
14 (*a*) R. T. Stibrany, J. Vasudevan, S. Knapp, J. A. Potenza, T. Emge and H. J. Schugar, *J. Am. Chem. Soc.*, 1996, **118**, 3980; (*b*) J. Vasudevan, R. T. Stibrany, J. Bumby, S. Knapp, J. A. Potenza, T. J. Emge and H. J. Schugar, *J. Am. Chem. Soc.*, 1996, **118**, 11676; (*c*) S. Knapp, J. Vasudevan, T. J. Emge, B. H. Arison, J. A. Potenza and H. J. Schugar, *Angew. Chem., Int. Ed.*, 1998, **37**, 2368.
15 M. P. O'Neil, M. P. Niemczyk, W. A. Svec, D. Gosztola, G. L. Gaines III and M. R. Wasielewski, *Science*, 1992, **257**, 63.
16 (*a*) R. W. Wagner and J. S. Lindsey, *J. Am. Chem. Soc.*, 1994, **116**, 9759; (*b*) R. W. Wagner, J. S. Lindsey, J. Seth, V. Palaniappan and D. F. Bocian, *J. Am. Chem. Soc.*, 1996, **118**, 3996.
17 R. van Grondelle, J. P. Dekker, T. Gillbro and V. Sundstrom, *Biochim. Biophys. Acta*, 1994, **1187**, 1.
18 (*a*) H. Michel, O. Epp and J. Deisenhofer, *EMBO J.*, 1986, **5**, 2445; (*b*) J. Deisenhofer and H. Michel, *Science*, 1989, **245**, 1463.
19 G. Feher, J. P. Allen, M. Y. Okamura and D. C. Rees, *Nature*, 1989, **339**, 111.
20 (*a*) P. Sayer, M. Gouterman and C. R. Connell, *J. Am. Chem. Soc.*, 1977, **99**, 1082; (*b*) C. J. Carrano and M. Tsutsui, *J. Coord. Chem.*, 1977, **7**, 79; (*c*) S. Mangani, E. F. Meyer, Jr., D. L. Cullen, M. Tsutsui and C. J. Carrano, *Inorg. Chem.*, 1983, **22**, 400; (*d*) C. A. Marrese and C. J. Carrano, *Inorg. Chem.*, 1983, **22**, 1858; (*e*) A. Harriman, *J. Photochem.*, 1983, **23**, 37; (*f*) H. Segawa, K. Kunimoto, A. Nakamoto and T. Shimidzu, *J. Chem. Soc., Perkin Trans. 1*, 1992, 939; (*g*) H. Segawa, A. Nakamoto and T. Shimidzu, *J. Chem. Soc., Chem. Commun.*, 1992, 1066; (*h*) T. Barbour, W. J. Belcher, P. J. Brothers, C. E. F. Rickard and D. C. Ware, *Inorg. Chem.*, 1992, **31**, 746; (*i*) Y.-H. Lin, C.-C. Lin, J.-H. Chen, W.-F. Zeng and S.-S. Wang, *Polyhedron*, 1994, **13**, 2887; (*j*) Y. H. Liu, M.-F. Bénassy, S. Chojnacki, F. D'Souza, T. Barbour, W. J. Belcher, P. J. Brothers and K. M. Kadish, *Inorg. Chem.*, 1994, **33**, 4480; (*k*) M.-T. Sheu, I.-C. Liu, P.-C. Cheng, C.-C. Lin, J.-H. Chen, S.-S. Wang and W.-F. Zeng, *J. Chem. Crystallogr.*, 1995, **25**, 231; (*l*) Y. Yamamoto, R. Nadano, M. Itagaki and K. Akiba, *J. Am. Chem. Soc.*, 1995, **117**, 8287; (*m*) T. A. Rao and B. G. Maiya, *Inorg. Chem.*, 1996, **35**, 4829.
21 (*a*) H. Segawa, K. Kunimoto, K. Susumu, M. Taniguchi and T. Shimidzu, *J. Am. Chem. Soc.*, 1994, **116**, 11193; (*b*) K. Susumu, K. Kunimoto, H. Segawa and T. Shimidzu, *J. Phys. Chem.*, 1995, **99**, 29.
22 (*a*) K. Susumu, K. Kunimoto, H. Segawa and T. Shimidzu, *J. Photochem. Photobiol. A: Chem.*, 1995, **92**, 39; (*b*) K. Susumu, H. Segawa and T. Shimidzu, *Chem. Lett.*, 1995, 929.
23 T. A. Rao and B. G. Maiya, *J. Chem. Soc., Chem. Commun.*, 1995, 939.
24 H. Segawa, N. Nakayama and T. Shimidzu, *J. Chem. Soc., Chem. Commun.*, 1992, 784.
25 J. Mason, *Multinuclear NMR*, Plenum Press, New York, 1987, pp. 369–402.

26 R. J. Abraham, G. R. Bedford, D. McNeillie and B. Wright, *Org. Magn. Reson.*, 1980, **14**, 418.
27 M. Kasha, H. R. Rawls and M. A. El-Bayoumi, *Pure Appl. Chem.*, 1965, **11**, 371.
28 T. Sauer, W. Caseri and G. Wegner, *Mol. Cryst. Liq. Cryst.*, 1990, **183**, 387.
29 (*a*) M. Zander and W. Rettig, *Chem. Phys. Lett.*, 1984, **110**, 602; (*b*) W. Rettig, *Angew. Chem., Int. Ed. Engl.*, 1986, **25**, 971; (*c*) W. Rettig, *Top. Curr. Chem.*, 1994, **169**, 253.
30 N. Mataga, H. Yao, T. Okada and W. Rettig, *J. Phys. Chem.*, 1989, **93**, 3383.
31 (*a*) S. R. Meech, A. J. Hoff and D. A. Wiersma, *Chem. Phys. Lett.*, 1985, **121**, 287; (*b*) S. G. Boxer, D. J. Lockhart and T. R. Middendorf, *Chem. Phys. Lett.*, 1986, **123**, 476; (*c*) S. G. Boxer, T. R. Middendorf and D. J. Lockhart, *FEBS Lett.*, 1986, **200**, 237; (*d*) S. R. Meech, A. J. Hoff and D. A. Wiersma, *Proc. Natl. Acad. Sci. U.S.A.*, 1986, **83**, 9464; (*e*) J. K. Gillie, B. L. Fearey, J. M. Hayes and G. J. Small, *Chem. Phys. Lett.*, 1987, **134**, 316; (*f*) D. J. Lockhart and S. G. Boxer, *Biochemistry*, 1987, **26**, 664; (*g*) D. J. Lockhart and S. G. Boxer, *Chem. Phys. Lett.*, 1988, **144**, 243; (*h*) L. M. McDowell, D. Gaul, C. Kirmaier, D. Holten and C. C. Schenck, *Biochemistry*, 1991, **30**, 8315.
32 (*a*) A. Warshel and W. W. Parson, *J. Am. Chem. Soc.*, 1987, **109**, 6143; (*b*) W. W. Parson and A. Warshel, *J. Am. Chem. Soc.*, 1987, **109**, 6152.

Paper 8/09840I